Equivalent Circuit Microwave Modeling of Graphene-loaded Thick Films Using S-parameters

ISSN 1590-8844
International Journal of Mechanics and Control, Vol. XX, No. YY, ZZZZ

SIMPLIFIED MODELS FOR MECHANICAL TRANSMISSION EFFICIENCY WITH OPPOSING AND AIDING LOADS

P. C. Berri M. D. L. Dalla Vedova P. Maggiore A. Manuello Bertetto

Dept. of Mechanical and Aerospace Engineering (DIMEAS), Politecnico di Torino, Turin, ITA

ABSTRACT

The computational power available for design of complex equipment is steadily increasing, allowing the use of very detailed models of the physical behaviour of the system. Nevertheless, in some situations simpler models are required. This is the case of preliminary sizing, when most of the system architecture is still to be defined in detail, and of monitoring routines intended to run in real-time, possibly with limited hardware resources available on-board a vehicle or embedded in equipment. With the emerging application of Prognostics and Health Management (PHM) to system design and development, simplified models of mechanical, hydraulic and electric equipment are becoming a key element to enable the implementation of fast and reliable algorithms for fault detection and estimation of remaining useful life. In this context, we address in particular the modelling of friction for mechanical parts. Variations from the nominal value of dry friction are usually among the early effects of wear and degradation of components: for example, a surface damage on a moving part can lead to an increase of the friction value, while the wear of a preloaded sealing can result in reduction in friction. Hence, in this work, we aim to develop accurate yet simple models for the efficiency of mechanical transmissions, which can be used within system level simulations intended to run in real-time for prognostic and monitoring tasks.

Keywords: Gear efficiency, Simplified model, Prognostics & Health Management (PHM), Dry friction

1 INTRODUCTION

Mechanical transmissions are commonly employed for the actuation of secondary flight controls of aircraft, either in combination with a hydraulic or electric centralized Power Drive Unit (PDU). This architecture is commonly employed to guarantee a symmetrical deflection of high lift devices (i.e. flaps and slats).
In fact, a failure in the flap actuation system leading to an asymmetrical deployment can easily result in the impossibility to balance the roll moment and control the aircraft. Hence, the symmetrical actuation is demanded to a highly reliable mechanical link that connects the aerodynamic surfaces to each other and to the PDU.
Several monitoring techniques have been developed to increase the reliability of these architectures and to deal with possible failures, mitigating their effects [1, 2].
Most strategies rely on sensors to detect anomalous behaviors of the system, in order to stop the actuation; other take advantage of more complex control logics to correct the asymmetry and regain some of the lost maneuverability.
Other emerging applications of mechanical transmissions in the aerospace field are related to the growing interest for electromechanical primary flight controls. Such technology is now employed only on small UAV platforms, but in the future it will enable the diffusion of More Electric Aircraft and All Electric Aircraft design philosophies [3, 4]. However, to counter the reliability issues of electromechanical systems PHM strategies will be necessary.
A prognostic approach to the design of such systems is aimed at identifying the early effects of common fault modes to estimate the Remaining Useful Life of the equipment and allow timely inspections and replacements. This would translate into an increase of system reliability and availability, as well into a reduction of maintenance and operating costs [5].
All these applications require simple yet detailed models of the system dynamics, accounting for a number of nonlinearities and off-nominal behaviors.
Among these effects, dry friction can be leveraged to infer the wear of several mechanical components such as bearings, gears, bushings, and linkages.

In this work we propose simplified models for the estimation of gear transmission efficiency. The models are required to correctly evaluate the behavior of mechanical systems subject to aiding and opposing loads, since aircraft actuators are commonly subject to either types of loads, in a mostly unpredictable pattern. Our models are intended to increase the accuracy of dynamic simulations of servosystems [6], without affecting noticeably the computational time. A first model is slightly more complex, and relies on a direct application of the Coulomb friction model [7-12]; this will be used as reference. A second model is more simplified and does not account for transmission architecture; only transmission ratio and a friction parameter are required, and this allows to estimate the behavior of equipment either early in the product development or when detailed data for off-the-shelf components is not available.

2 REFERENCE MODEL

The first model we consider is a direct application of the Coulomb friction on the transmission geometry. The considered mechanical transmission, in a first application for validation purpose, is a single cylindrical gearing with involute tooth profile, module m, and pressure angle θ. The transmission ratio is $R = z_2/z_1$, where z_1 and z_2 are the numbers of teeth of the motor and driven gears respectively. Referring to Figure 1:

- $r_p = mz$ is the pitch radius of each wheel;
- $r_t = r_p + a$ is the top radius of each wheel, where a is the addendum;
- $r_b = r_p \cos\theta$ is the base radius of each wheel.

A force F is exchanged between the two wheels along the segments A and B, which lie onto the line of action, tangent to both base circles. A and B are bounded by the top circles of the two wheels and separated by the pitch circles.
The length of segments A and B is respectively:

$$A = \sqrt{r_{t1}^2 - r_{b1}^2} - d_{p1} \quad (1)$$

$$B = \sqrt{r_{t2}^2 - r_{b2}^2} - d_{p2} \quad (2)$$

where $d_p = r_p \sin(\theta)$. Considering an opposing load condition, the motor wheel turns clockwise, and the driven wheel turns counterclockwise. As a result, the teeth surfaces slide towards each other along B, and slide away from each other along A.
We assume that the force F is constant along the whole contact segment. Then, we can consider the friction force to be constant in modulus, perpendicular to the line of action, and directed in the direction opposite to the sliding velocity.
The resulting torque acting on the motor wheel is:

$$T_{M,D} = Fr_{b1} - \frac{fFB}{A+B}\left(d_{p1} - \frac{B}{2}\right) + \frac{fFA}{A+B}\left(d_{p1} + \frac{A}{2}\right) + \rho_1\sqrt{F^2 + \left(fF\frac{A-B}{A+B}\right)^2} \quad (3)$$

Similarly on the driven wheel:

$$T_{U,D} = Fr_{b2} - \frac{fFB}{A+B}\left(d_{p2} + \frac{B}{2}\right) + \frac{fFA}{A+B}\left(d_{p2} - \frac{A}{2}\right) - \rho_2\sqrt{F^2 + \left(fF\frac{A-B}{A+B}\right)^2} \quad (4)$$

where f is the tooth-tooth friction coefficient and ρ is the friction radius of the bearings holding the gears. The subscript D denotes the opposing load (direct) condition. The transmission efficiency in this condition can be computed as:

$$\eta_D = \frac{1}{R}\frac{T_{U,D}}{T_{M,D}} \quad (5)$$

In the aiding load (inverse) condition we can consider the same forces distribution as the previous case.

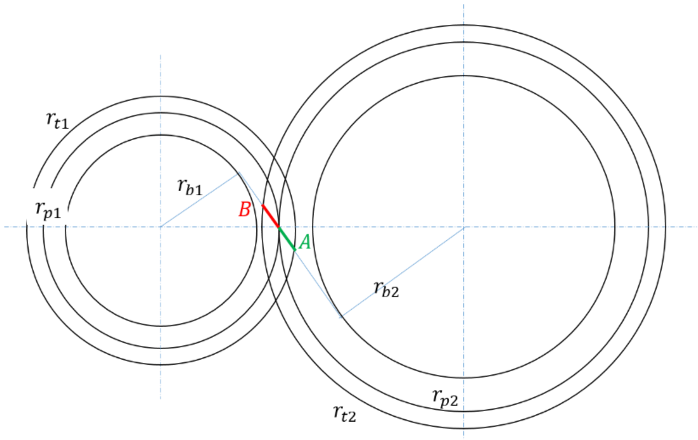

Figure 1 Reference gear geometry

The velocity is reversed, so the friction forces are inverted as well. Then we can express the torques acting on the two wheels as:

$$T_{M,I} = Fr_{b1} + \frac{fFB}{A+B}\left(d_{p1} - \frac{B}{2}\right) - \frac{fFA}{A+B}\left(d_{p1} + \frac{A}{2}\right) - \rho_1\sqrt{F^2 + \left(fF\frac{A-B}{A+B}\right)^2} \tag{6}$$

$$T_{U,I} = Fr_{b2} + \frac{fFB}{A+B}\left(d_{p2} + \frac{B}{2}\right) - \frac{fFA}{A+B}\left(d_{p2} - \frac{A}{2}\right) + \rho_1\sqrt{F^2 + \left(fF\frac{A-B}{A+B}\right)^2} \tag{7}$$

This allows to get the expression of the efficiency for the aiding load condition:

$$\eta_I = R\frac{T_{M,I}}{T_{U,I}} \tag{8}$$

3 SIMPLIFIED MODEL

The second model considered is further simplified to account only for easily available data, i.e. the transmission ratio. The main assumption, which will be verified in the results section, is to suppose that the relationship between aiding load efficiency and opposing load efficiency is not significantly influenced by the particular architecture of the transmission, but only by the transmission ratio.
Under this assumption, we derive the relationship between η_D, η_I and R for the most simple transmission possible, that is, a lever with friction in the pivot point (Figure 2). We define the friction radius ρ and the transmission ratio $R = l_2/l_1$, where l_1 and l_2 are the distances between the pivot point and the motor force (F_M) and load force (F_U).
In the opposing load condition, the hinge reaction is applied closer to the motor force, so the equilibrium equation can be written as:

$$F_{U,D} = F_{M,D}\frac{l_1 - \rho}{l_2 + \rho} \tag{9}$$

and the mechanical efficiency is:

$$\eta_D = \frac{1}{R}\frac{F_{U,D}}{F_{M,D}} = \frac{1}{R}\frac{R-u}{1+u} \tag{10}$$

where $u = \rho/l_2$ is a friction parameter. In the aiding load condition the velocity is reversed, so the hinge reaction is applied on the opposite side of the pivot point:

$$F_{U,I} = F_{M,D}\frac{l_1 + \rho}{l_2 - \rho} \tag{13}$$

$$\frac{1}{\eta_I} = \frac{1}{R}\frac{F_{U,I}}{F_{M,I}} \Rightarrow \eta_I = R\frac{1-u}{R+u} \tag{14}$$

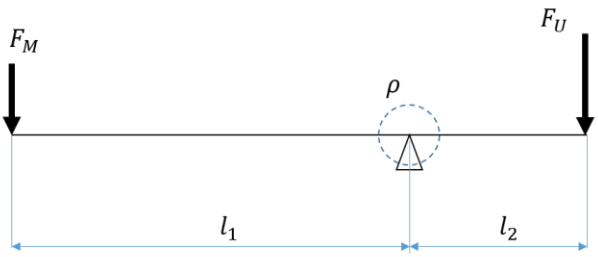

Figure 2 Simplified transmission geometry.

Solving equation (10) for u and substituting into equation (12), it is possible to determine the relationship between η_D, η_I and R:

$$u = \frac{R - R\eta_D}{R\eta_D + 1} \tag{13}$$

$$\eta_I = \frac{2R^2\eta_D - R^2 + R}{R^2\eta_D + R - \eta_D + 1} \tag{14}$$

For high values of the transmission ratio R, the aiding load efficiency approaches zero as the opposing load efficiency approaches 50%, in accord to [13-15].

4 RESULTS

The simplified model provides a relationship between opposing load efficiency, aiding load efficiency, and transmission ratio, regardless of the particular configuration of a given mechanical transmission. Figure 3 shows the surface plot of the simplified model, for a transmission ratio ranging from 0.1 to 50. In Figure 3, the shown efficiencies range from 1 to -1 for clarity and readability; however, conservation of energy only poses an upper bound to efficiency at 1, since a negative efficiency value means that the motor shall produce a positive work even in the aiding load condition.
The reference model depends on multiple parameters, such as dynamic friction values, gear geometry and bearing characteristics. Then, a surface plot cannot be built like for the simplified model. To compare the results of the two models, we perform a sampling in the space of the independent parameters of the reference model $\{z_1, z_2, \rho_1, \rho_2, F, m, \theta\}$. A total of 500 combinations of the parameters are computed with a random sampling, with a logarithmic distribution in z_1 and z_2, and a constant distribution in the other variables. In order to explore the same domain represented in Figure 3, some of the parameters are bounded in a larger range than that found in common applications. Specifically, the number of teeth of the driven wheel can be as high as 3000, to achieve a high transmission ratio with a single stage configuration. In addition, the values of contact dry friction between the teeth and the friction radii of the bearings are allowed to grow to high values, in order to analyze irreversible configurations that otherwise could not be achieved with a single stage, cylindrical gear reducer.

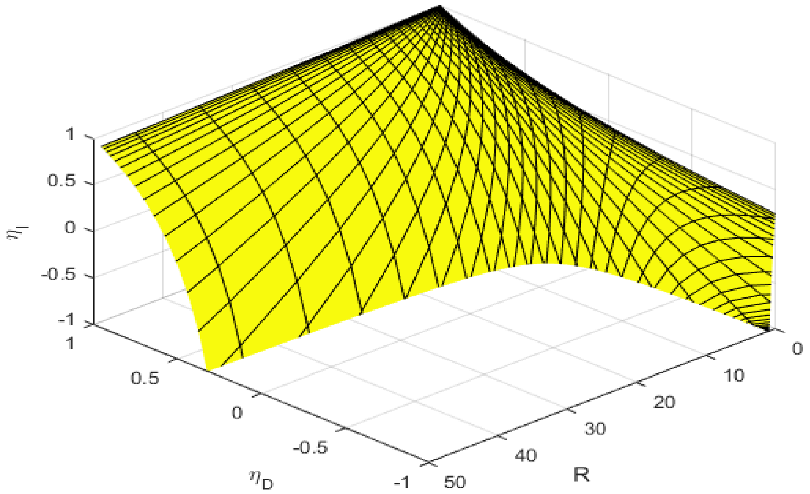

Figure 3 Surface plot of equation (14).

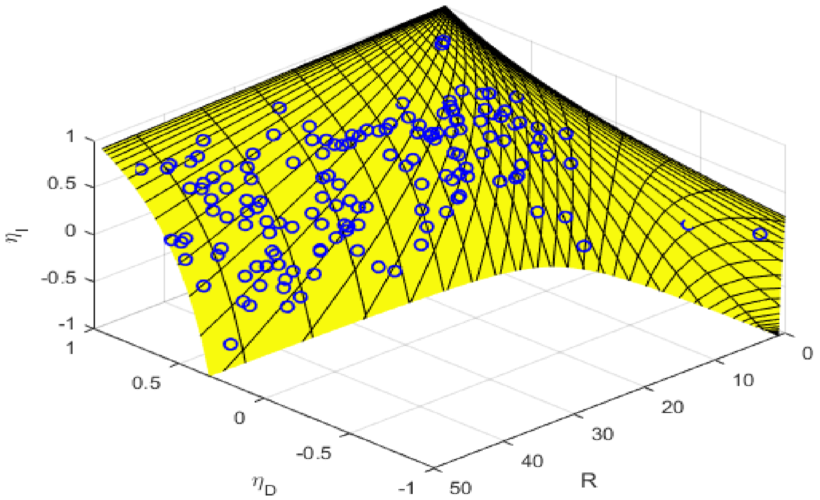

Figure 4 Comparison between the two models. The blue circles are the data points computed with the reference model.

Figure 4 shows the comparison between the two models, by plotting the results of the reference model over the surface plot of the simplified model. For each data point of the reference model, we compute the absolute errors in η_D and η_I of the simplified model with respect to the reference model.

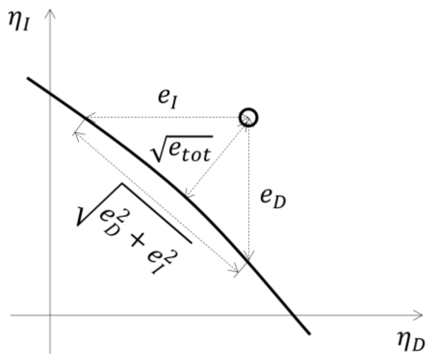

Figure 5 Graphical representation of the derivation of total error. The solid curve is the simplified model, the circle is the reference model data point.

A total squared error is evaluated as the square of the normal distance between the $\eta_D - \eta_I$ curve of the simplified model for a given gear ratio, and the data point of the reference model (Figure 5 [16, 17]). The expression of the total squared error is then:

$$e_{tot} = \left(\frac{e_I e_D}{\sqrt{e_D^2 + e_I^2}} \right)^2 \qquad (15)$$

Figure 6 shows the statistical distribution of the total squared error, and highlights how it is usually in the order of 10^{-2}, corresponding to absolute errors less than 10% in the estimated efficiencies.

5 CONCLUSIONS

Two models with different level of detail for the efficiency of mechanical transmissions were developed and compared. Both are able to deal with opposing load and aiding load conditions, which is a necessary requirement for accurate transmission models of electromechanical servoactuators.

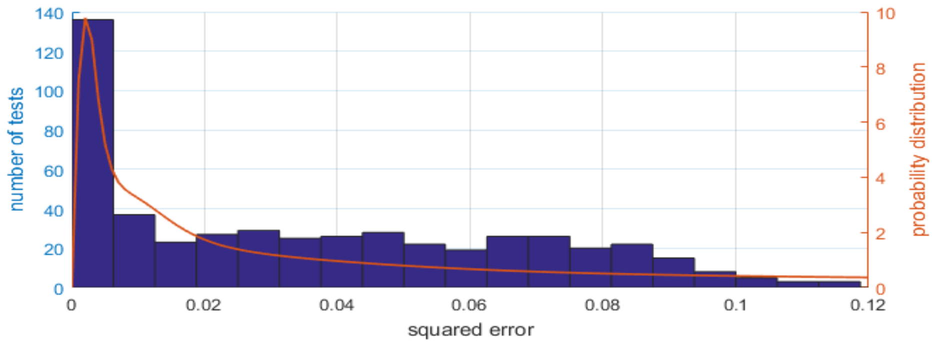

Figure 4 Distribution of the total squared error between the two models.

The second, simplified model is developed in order to give an estimate of the transmission behavior without needing detailed information about its architecture and configuration. Thus, this model can be employed in preliminary sizing or to estimate performances of mechanical transmissions from the available datasheet, when only limited information is available. The comparison between the two models showed that the results of both simulations are compatible with each other, despite the very different modelling approach.
Further work is needed to extend the reference model to different architectures, such as multi-stage gearboxes, planetary reducers, or different gear geometry (e.g. helical, bevel, or worm gears), and to determine if the simplified model is applicable to these configurations. Additionally, higher fidelity data, either from an experimental campaign or from FE/multibody analyses, is required to validate the models.

REFERENCES

[1] Borello, L. and Villero, G. and Dalla Vedova, M.D.L., Flap failure and aircraft controllability: Developments in asymmetry monitoring techniques. *Journal of Mechanical Science and Technology*, Vol. 28, No. 11, pp. 4593-4603, 2014. doi: 10.1007/s12206-014-1027-0

[2] Borello, L. and Villero, G. and Dalla Vedova, M., New asymmetry monitoring techniques: Effects on attitude control. Aerospace Science and Technology, Vol. 13, No. 8, pp. 475-487, 2009.

[3] Maré, J.-C., Electro-mechanical Actuators. *Aerospace Actuators 2*, J. Wiley & Sons, Inc., pp. 171–217, 2017.

[4] Garriga A.G., Ponnusamy, S.S., and Mainini L., A multi-fidelity framework to support the design of More-Electric Actuation. *Proc. of the 2018 Multidisciplinary Analysis and Optimization Conference, AIAA Aviation Forum*, (AIAA 2018-3741), 2018.

[5] Vachtsevanos G., Lewis F., Roemer M., Hess A., and Wu B., *Intelligent Fault Diagnosis and Prognosis for Engineering Systems*, John Wiley & Sons, Inc., 2006.

[6] Borello, L. and Dalla Vedova, M.D.L., A dry friction model and robust computational algorithm for reversible or irreversible motion transmissions. *International Journal of Mechanics and Control*, Vol. 13, No. 2, pp. 37-48, 2012.

[7] D. Karnopp, Computer simulation of stick-slip friction in mechanical dynamic systems. *J. Dyn. Systems, Meas. & Control*, Vol. 107, No. 1, pp. 100-103, 1985.

[8] D. Quinn, A new regularization of Coulomb friction. *J. of Vibration and Acoustics*, Vol. 126, No. 3, pp. 391-397, 2004.

[9] De Martin A., Dellacasa A., Jacazio G. and Sorli M., High-fidelity model of electro-hydraulic actuators for primary flight control systems. *Proc. Of the BATH/ASME 2018 Symposium on Fluid Power and Motion Control, FPMC 2018*, 2018.

[10] Pennestrì, E. and Rossi, V. and Salvini, P. and Valentini, P.P., Review and comparison of dry friction force models. *Nonlinear Dynamics*, Vol. 83, No. 3, pp. 1785-1801, 2016. doi 10.1007/s11071-015-2485-3

[11] Kikuuwe R., Takesue N., Sano A., Mochiyama H., Fujimoto H., Fixed-step friction simulation: from classical coulomb model to modern continuous models. *Proc of the International Conf. on Intelligent Robots and Systems IEEE/RSJ 2005*, pp. 3910-3917, 2005.

[12] Dupont P., Armstrong B. and Hayward V., Elasto-plastic friction model: contact compliance and stiction. *Proc. of American Control Conf.*, Vol.2, pp. 1072-1077, 2000.

[13] Tonoli A., Amati N., Impinna F., Girardello Detoni J., Ruzimov S., Gasparin E. and Abdivakhidov K., Influence of Dry Friction on the Irreversibility of Cycloidal Speed Reducer. *Proc. of World Tribology Congress*, Turin (Italy), 2013.

[14] Tuplin W.A., The Limitations of Epicyclic Gears. *Machine Design*, Vol. 30, pp. 124-126, 1964.

[15] Salgado D. R. and Del Castillo J. M., Conditions for Self-Locking in Planetary Gear Trains. *J. Mechanical Design*, Vol. 129, No. 9, pp. 960-968, 2007.

[16] Markovsky I. and Van Huffel S., Overview of total least-squares methods. *Signal Processing* Vol. 87, pp. 2283–2302, 2007.

[17] Berri P.C., Dalla Vedova M.D.L. and Maggiore P. On-Board Electromechanical Servomechanisms Affected by Progressive Faults: Proposal of a Smart GA Model-Based Prognostic Approach. *Safety and Reliability – Theory and Applications*, 2017.